frontiers in Astronomy and Space Sciences

TYPE Original Research
PUBLISHED 15 July 2026
DOI 10.3389/fspas.2026.1812284

OPEN ACCESS

EDITED BY
Abhishek Kumar Srivastava,
Indian Institute of Technology
(BHU), India

REVIEWED BY
Juie Shetye,
New Mexico State University,
United States
Pradeep Kayshap,
VIT Bhopal University, India

*CORRESPONDENCE
S. D. T. Grant,
samuel.grant@qub.ac.uk

RECEIVED 16 February 2026
REVISED 21 May 2026
ACCEPTED 31 May 2026
PUBLISHED 15 July 2026

CITATION
Grant SDT, Berretti M, Chambers G, Jess DB, Stangalini M, Jafarzadeh S, Smitha HN and Berrilli F (2026) Probing oscillations in the lower solar atmosphere with the FRANCIS integral field unit.
Front. Astron. Space Sci. 13:1812284.
doi: 10.3389/fspas.2026.1812284

Probing oscillations in the lower solar atmosphere with the FRANCIS integral field unit

S. D. T. Grant[1]*, M. Berretti[2,3], G. Chambers[1], D. B. Jess[1,4], M. Stangalini[5], S. Jafarzadeh[1], H. N. Smitha[6] and F. Berrilli[3]

[1]Astrophysics Research Centre, School of Mathematics and Physics, Queen's University Belfast, Belfast, United Kingdom, [2]Department of Physics, University of Trento, Trento, Italy, [3]Department of Physics, University of Rome Tor Vergata, Rome, Italy, [4]Department of Physics and Astronomy, California State University Northridge, Los Angeles, CA, United States, [5]ASI Italian Space Agency, Rome, Italy, [6]Max Planck Institute for Solar System Research, Göttingen, Germany

The photosphere is dominated by 3 mHz oscillations, and as we move upward through the solar atmosphere, the dominant frequency is progressively filtered up to 5 mHz, which is commonly observed ubiquitously in the chromosphere. However, the interaction of these waves with magnetic fields often leads to conversions, reflections, and the formation of standing modes, making their interpretation much more complex. In this paper, we study wave propagation in the lower solar atmosphere using the newly developed FRANCIS instrument, a fibre-fed integral field unit capable of capturing simultaneous, multi-line, high-resolution observations. We selected nine fibres representative of distinct magnetic populations of the active region to study their refined global wavelet spectra at 21 heights between ~10 – 400 km. The results reveal that different areas of the same active region behave in strikingly different ways, with notable differences in the frequency barycentre of 3.6 – 6.92 mHz across magnetic regions, highlighting the importance of future studies on spatial variability and its link to other plasma parameters.

KEYWORDS
chromosphere, integral field unit spectroscopy, MHD waves, photosphere, wave propagation

1 Introduction

It is well-known that magnetic structures in the solar atmosphere host a plethora of wave modes. The observed oscillations span a wide range, from magnetoacoustic modes resulting from mode conversion (Spruit and Bogdan, 1992; D'Silva, 1994; Cally et al., 1994) to purely MHD modes driven by resonances (Spruit, 1981; Edwin and Roberts, 1982; 1983; Zhugzhda, 1984; Roberts, 2019; Stangalini et al., 2021). These structures then act as conduits (Giovanelli et al., 1978; Lites and Thomas, 1985), guiding these waves into the upper layers of the solar atmosphere providing an additional source of energy (e.g., Krishna Prasad et al., 2015; 2017). Therefore, these oscillations are essential for a better understanding of local plasma conditions and the Sun's atmospheric energy balance, and may help resolve long-standing problems in solar physics such as coronal heating (Goossens et al., 2013; Doorsselaere et al., 2020) and solar wind acceleration (Pontieu et al., 2007).

Following the pioneering works of Kneer et al. (1981), Lites (1984), Lites (1986), propagating waves in the solar atmosphere have been observed across a wide range of scenarios (Lites, 1992; Bogdan, 2000; Socas-Navarro et al., 2000; Rosenthal et al., 2002; Bogdan et al., 2003; Bogdan and Judge, 2006; Khomenko et al., 2008; Vigeesh et al., 2011; Fedun et al., 2011; Dorotovič et al., 2014; Grant et al., 2015; Jafarzadeh et al., 2017; Kayshap et al., 2018; Kayshap et al., 2020; Bahauddin et al., 2024, to name a few). Specifically, in Centeno et al. (2006), the authors used spectropolarimetric observations in the near-IR spectral region to study the properties of umbral line-of-sight (LOS) velocity signals from the photosphere to the chromosphere. In their work, they show observational evidence of waves with frequencies above the acoustic cut-off propagating upwards from the photosphere. Subsequent studies, such as Centeno et al. (2009), verified this behavior across a range of magnetic features verifying its ubiquity across the lower solar atmosphere. Furthermore, in Gilchrist-Millar et al. (2021), the authors investigated a cluster of magnetic pores and showed evidence of propagating body and surface modes by examining the Si I 1082.7 nm line bisector velocities, observed with the Facility Infrared Spectropolarimeter (Jaeggli et al., 2010) at the Dunn Solar Telescope (DST). In a follow-up work by Grant et al. (2022), the authors complemented the same dataset with Ca II 854.2 nm observations obtained with the Interferometric BIdimensional Spectropolarimeter (Cavallini, 2006) mounted at the DST. Again, they studied the bisector velocities and showed clear evidence of waves propagating in the chromosphere.

In Jess et al. (2013), the authors studied the impact of magnetic field inclination on the propagation of waves in the chromosphere. Using data obtained from both the Rapid Oscillations in the Solar Atmosphere (ROSA; Jess et al., 2010) and the Hydrogen-Alpha Rapid Dynamics camera (HARDcam; Jess et al., 2012) imagers at the DST, Jess et al. (2013) showed for the first time how the distribution of dominant frequencies in the upper layers of the solar atmosphere is closely linked to the magnetic field topology in the photosphere (see also Löhner-Böttcher and Bello González (2015); Löhner-Böttcher et al. (2016). Furthermore, in Stangalini et al. (2021), the B-ω was introduced, providing an effective way to show the sometimes drastic changes within different regions of the same sunspot, even at the same atmospheric height.

Moreover, the sharp density and temperature gradients often observed at photospheric and chromospheric heights can act as mirrors for waves, leading to partial reflection (Mein and Mein, 1976; Provost and Mein, 1979; Jefferies et al., 1997; Moretti et al., 2007; Khomenko and Collados, 2009; Rijs et al., 2015; Jefferies et al., 2019). In Fleck and Deubner (1989), the authors provided strong observational evidence for the first time of standing acoustic waves in the chromosphere, resulting from a reflective layer at the transition region. Recently, in Chaturmutha et al. (2024), the authors studied the propagation of waves in the photosphere and low-chromosphere using data captured with both the Solar Dynamics Observatory's Helioseismic and Magnetic Imager (SDO/HMI; Pesnell et al., 2012; Schou et al., 2012) and the Magneto-Optical filters at Two Heights (MOTH; Forte et al., 2018) and found compelling evidence for wave reflection by comparing the measured phase travel time with wave propagation models that also include reflection. Through their analysis, the authors are also capable of estimating the acoustic cut-off frequency and the radiative cooling times, further highlighting the need for multi-wavelength studies to improve our knowledge of the solar atmosphere.

However, a clearer understanding of wave propagation in the solar atmosphere can only be achieved through simultaneous, multi-line observations at high spatial resolution and rapid temporal cadence. To this end, there have been a number of advancements in the development of Integrated Field Units (IFUs; see the review by Iglesias and Feller (2019)) suitable for solar physics. Unlike traditional instruments that record either a two-dimensional image (like a filter-based imaging system) or spectra spanning a single spatial dimension (like conventional slit-based spectrographs), an IFU is able to perform spectroscopy of multiple spatial locations simultaneously by reformatting the two-dimensional spatial domain using either fibres, mirrors, or microlens arrays, before passing the light through a conventional spectrograph. Once remapped back into the spatial domains, this provides a time series of spectra, i.e., data of the form (x, y, λ, t). In this work, we showcase the capabilities of IFUs in solar physics, thanks to the Fibre-Resolved opticAl and Near-ultraviolet Czerny-Turner Imaging Spectropolarimeter (FRANCIS; Jess et al., 2023a), a novel IFU mounted at the DST that observed the Sun in the near-ultraviolet to mid-optical wavelength range. In particular, we studied the LOS velocity of 20 different spectral lines between 580.758 nm and 597.250 nm, spanning nearly 400 km of the Sun's atmosphere from $z \approx 10$ km above the temperature minimum up to $z \approx 380$ km.

2 Dataset and methods

The data used in this work were obtained with FRANCIS, a fibre-bundle based IFU with 400 total fibres in a 20×20 hexagonal packing configuration. The data cube considered was observed between 18:03–18:39 UTC on 2022 August 29 under excellent seeing conditions, with an overall wavelength coverage spanning 580.758 – 597.250 nm and a sampling of 0.008 nm pixel^{-1} and a spectral imaging cadence of 2 s. The 30×30 arcsec^2 field of view covers part of the sunspot group within NOAA active region 13,089, offering the chance to study umbral, penumbral, and plage regions within the AR. In Figure 1, we show a ROSA G-Band image with the FRANCIS field of view (FoV) superimposed (panel a). The coloured dots highlight the fibres studied in this work, representing a sample of typical features found within an active region. The selected fibres comprise three different plage areas, the umbral core, the penumbra, and the umbra-penumbra boundary and split parts of the umbra. The characteristic observables of these regions are presented in Table 1.

From the full range of wavelengths observed by FRANCIS, we selected 23 spectral lines with significant absorption depths to allow for comparison with those catalogued in the solar atlas spectrum (BASS 2000, 2001). For more information on the selected lines, along with the reference wavelength and corresponding ion, we refer the reader to Table 2.

The lines considered exhibit a variety of spectral line dynamics and evolution (e.g., variable line shapes, asymmetries, and widths) that preclude line fitting through simple methods such as Gaussian fits. For instance, Chambers et al. (2026) utilized precision Voigt fits from the `LineFit` software (Jafarzadeh et al., 2026) to generate velocity time series from the more chromospheric Na I D_1/D_2 lines observed in the FRANCIS data. In order to estimate the

10.3389/fspas.2026.1812284

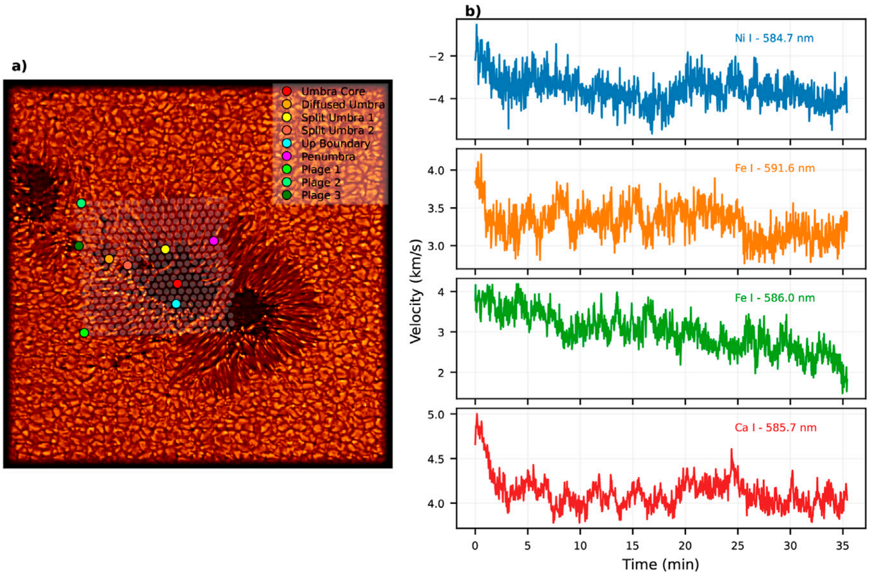

FIGURE 1
Overview of the FRANCIS observations. **(a)** ROSA G-Band snapshot of AR 13089, where the superimposed dots highlight the FRANCIS field of view and different coloured dots represent isolated regions of the FoV. **(b)** Raw sample time-series for different wavelengths of the umbral core. From top to down respectively Ni I 584.7 nm, Fe I 591.6 nm, Fe I 586.0 nm and Ca I 585.7 nm.

TABLE 1 **Per-fibre properties: distance from the umbral magnetic barycenter (d), mean HMI line-of-sight magnetic field $\langle B_{LOS}\rangle$, and mean HMI continuum intensity $\langle I\rangle_{HMI}$ given as a fraction of the umbral core intensity I_{umb}.**

Fibre	Group	d [arcsec]	d [Mm]	$\langle B_{LOS}\rangle$ [G]	$\langle I\rangle_{HMI}$ [I_{umb}]
148	Umbra core	0.00	0.00	−1081	1
244	Split umbra 1	5.07	3.67	−1044	1.29
88	Split umbra 2	3.33	2.41	−1036	1.16
232	U-P boundary	9.43	6.84	−830	1.37
257	Penumbra	9.81	7.11	−608	1.75
39	Plage 1	8.28	6.01	−443	1.82
212	Plage 2	7.12	5.16	−594	1.8
275	Plage 3	15.87	11.51	−549	1.69

Doppler velocity signals from every fiber of every selected spectral line observed by FRANCIS in a consistent manner, we used the well-established Fourier phase-based method, which is similar to a Fourier tachometer (Schlichenmaier and Schmidt, 2000). This method is independent of profile shape, instead converting the intensity of the profile within a wavelength window into Fourier space, producing frequencies each with a defined phase. The line profile shift due to Doppler motion equates to a linear change in the phase, particularly in the fundamental harmonic as it is strong and stable. In practice, we infer the Doppler shift from the phase of the fundamental Fourier harmonic within a manually selected wavelength window that captures the main absorption feature while excluding blends or secondary minima, which could otherwise bias the phase-derived velocity. This phase shift is then converted to a wavelength shift that can be used to calculate the line-centre wavelength, line-core intensity, and line-of-sight velocity (v_{LOS}) of the plasma through,

$$v_{LOS}(t) = \frac{\lambda_i(t) - \lambda_{ref}}{\lambda_{ref}} \cdot c,$$

where $\lambda_i(t)$ is the measured wavelength position of the line core at frame t, λ_{ref} is the reference wavelength of the selected spectral line, and c is the speed of light. An example of the observed line-of-sight velocity time-series is shown in Figure 1b for four different wavelengths of the umbral core fiber. Further information on the Fourier tachometer method can be found in the applications by Evans (1981), Brown (1986) and Jones (1989) that verify its validity and robustness.

Typically the reference wavelength representing the line-core wavelength at rest in v_{LOS} calculations is deduced by fitting an

TABLE 2 Spectral lines and their formation heights. Wavelengths are given in nm and heights in km. The reference wavelength corresponds to the rest wavelength taken from the solar atlas, while the peak wavelength indicates the position of the spectral peak as observed by FRANCIS.

Ref. Wavelength [nm]	Peak wavelength [nm]	Ion	FAL-C HoF [km]	Umbral HoF [km]
581.6381	581.6335	Fe I	227.5	−498.4
584.7000	584.6937	Ni I	111.5	−448.6
584.8124	584.8132	Fe I	147.1	−490.1
585.2223	585.2276	Fe I	102.4	−521.7
585.3684	585.3631	Ba II	318.4	−359.5
585.5081	585.5304	Fe I	36.9	−527.9
585.6092	585.6101	Fe I	93.5	−502.1
585.7461	585.7456	Ca I	369.7	−262.2
585.9593	585.9608	Fe I	279.8	−432.6
586.2367	586.2317	Fe I	336.3	−363.7
586.6457	586.6461	Ti I	178.6	−208.9
586.7564	586.7497	Ca I	195.3	−310.8
588.3824	588.3834	Fe I	217.1	−478.7
589.2882	589.2759	Ni I	25.9	−374.2
590.1460	590.1445	Fe I	197.9	−545.2
590.5684	590.5669	Fe I	197.9	−473.6
591.4207	591.4196	Fe I	312.2	−385.2
591.6254	591.6188	Fe I	204.2	−360.4
593.0191	593.0214	Fe I	289.3	−446.8
593.4663	593.4676	Fe I	255.9	−463.8
595.6701	595.6592	Fe I	220.3	−354.3

average quiescent profile in the field-of-view (e.g., Grant et al., 2015; 2022). This is not feasible for the variety of spectral lines considered, so the reference wavelength is taken from the solar atlas spectrum (see Table 2). This can introduce uncertainty to the absolute velocity values, as there is no correction for solar disk position, and in comparison between spectral lines as seen in Figure 1, though this has no influence on v_{LOS} oscillation studies as these time-series are always first detrended so only perturbations about the global background trend are considered. Care must also be taken with the tachometer method to include as many wavelength points as possible whilst avoiding additional minima in the line profile (e.g., caused by spectral line blends). This is achieved through manual selection of the wavelength regions and ensures no erroneous signals are included.

To provide context for the many spectral lines included in the sample, particularly those not extensively studied, we estimated their formation heights in distinct atmospheric regions. In particular, we focus on the quiescent magnetic conditions to provide a first-order comparison with other studies, as well as qualitatively estimating the formation height within a sunspot umbra to better contextualize the results of this study. In both cases, the Eddington-Barbier (EB; Rutten, 2021) approximation is utilized to provide the geometric height associated with the $\tau_\lambda = 1$ representation of the visible surface without need of intensive computations. For the quiescent conditions, the one-dimensional FAL-C model (Fontenla et al., 1993) is used, with umbral formation heights generated as a weighted average of a 20×20 pixel^2 central umbral region free of umbral dots from the MuRAM simulation of Rempel (2012), see Smitha et al., 2023 for further details. The height of formation (HoF) for each line are presented in Table 2 and represent an approximation of their height ordering. There are limitations to the models applied, such as FAL-C being one-dimensional and the region extracted from the umbral simulation showing expected variance due to the Wilson depression (Solanki, 2003), although each spectral line exhibited a similar standard deviation in formation height across the region (30 – 40 km) indicating self-consistency across the umbral height estimations considered. Similar uncertainties will always be present in the physical formation heights of any observation due to the unique response of spectral lines to changes in temperature, velocity, ionization, and opacity. We therefore present these formation heights to orient the lines to more familiar atmospheric diagnostics and confirm that these lines form in the upper photosphere, alongside providing the opportunity for approximate atmospheric layering of the observables. We emphasise that this ≈30–40 km spread reflects local variability of the EB $\tau_\lambda = 1$ proxy within that umbral atmosphere, rather than a full radiative-transfer formation-height uncertainty (i.e., contribution-function width). We also note that our primary conclusions rely on relative comparisons across fibres/regions and on the ensemble of lines, rather than on the exact absolute height of any single line; nevertheless, the EB heights provide a physically motivated ordering within the upper photospheric range.

3 Results

To obtain a reliable estimate of the power spectral density of LOS velocity oscillations, we followed the procedure highlighted in Jess et al. (2023b) and Jafarzadeh et al. (2025). We computed the Refined Global Wavelet Spectrum (RGWS) directly on the total duration of the observations ($T = 2126$ s), using a Morlet wavelet and a confidence level above 95%. This approach ensures a variable frequency resolution that scales logarithmically, providing better resolution in the low-frequency domain, which is vital as the short duration of the observation window produces a coarse frequency sampling of 0.47 mHz, necessitating optimization. Moreover, the RGWS, as opposed to other traditional techniques like FFT and Welch, allows us to focus on statistically significant power above the confidence level threshold, granting a more robust comparison between fibres and heights. By utilising the full 2 s cadence, we maintained the Nyquist frequency at 250 mHz, which is far above the frequencies of interest, reducing concerns about aliasing into the frequency band of interest. To minimise the impact of time-series truncation, we linearly detrended the data and apodized it using a Tukey window with $\alpha = 0.1$. The position of the selected fibres is shown in Figure 1, overlaid on a ROSA G-Band image of the observed AR, with differently coloured dots highlighting the FRANCIS fibres layout.

Figures 2, 4 display the RGWS as a function of height for the six umbral and three plage (quiescent) fibres, respectively. From inspection of the magnetised regions in Figure 2, there is a variety of frequency contributions to the power spectra, with multiple umbral components exhibiting high frequency power above the expected 3 – 5 mHz range. Wave power morphology was initially considered through analysis of dominant frequencies, which can isolate the effects of height stratification (e.g., Jafarzadeh et al., 2021; Kayshap et al., 2025). Figure 3 exhibits the two behaviours seen amongst the regions. In the case of the penumbral and quiescent plasma, there is no noticeable shift in the dominant frequency. This is also the case in magnetic regions such as the umbral core, however the higher frequency power presents as dominant in certain lines which makes trends difficult to identify. In order to best encapsulate the range of frequency distributions between spectral observations of the same region, we employ frequency-weighted mean power to calculate the frequency barycenter. We rely on our calculation of the frequency barycenter to not exclude high frequency power that remains below that of the 3 – 5 mHz window.

The umbral core in Figure 2a best represents the diverse frequency distribution of wave power. The dominant frequency of the majority of spectral lines remains within the 3 – 4 mHz band expected of photospheric observations, however, higher frequency power produces an average frequency barycentre with a standard deviation of 5.32 ± 0.77 mHz, with the barycentre ranging from 4.26 – 6.92 mHz. This behavior is also clearly seen at the umbra-penumbra boundary (4.92 ± 0.70 mHz) and within the second split umbra (4.90 ± 0.76 mHz). These high-frequency signatures are consistent with harmonics of the p-mode frequencies, implying that these magnetic regions are comprised of vertical fields allowing standing modes and wave reflection to manifest via interactions with the photosphere-chromosphere boundary and/or a chromospheric cavity (Jess et al., 2021a). This is consistent with the lack of harmonic power in the penumbral spectra, consistent with more inclined field geometry in penumbral regions (e.g., Jess et al., 2013), where wave propagation and mode coupling can differ from the more vertical umbral field. It also implies that the first split umbra and diffused umbra have inclined magnetic components that inhibit bulk wave reflection.

When considering the height distribution of wave power there appears a more complex scenario than previous studies. Investigations concerned with frequency distributions across the photosphere-chromosphere boundary, such as Grant et al. (2022) and Kayshap et al. (2025), were able to resolve a clear shift to higher frequencies as a function of height. Some of the magnetic regions do show a general trend of increasing frequency barycenter, such as the first split umbra, penumbra, and diffused umbra (Figures 2c,e,f), although the stronger magnetic regions are not as clear. Regardless of the contributions of harmonic power, by observation the dominant 3 – 4 mHz shows little morphology with height, even with the extra-ordinary core umbral signature of Fe I 590.1 nm excluded that exhibits little p-mode power.

In contrast to the variable presentation of wave power within the sunspot, the three plage fibres behave uniformly. Here, the 3 – 4 mHz band (typically associated with p-modes) is much more consistent than in the sunspot fibers, with a frequency barycenter of 3.80 ± 0.40 mHz. There is also only a small contribution of higher frequency power, allowable with the variety of magnetic configurations expected within plage. The lack of clear transition from 3 mHz towards 5 mHz in the quiet Sun acoustic oscillations seen in other works (Jess et al., 2023b) implies that the height range sampled is not sufficiently large to sample the photosphere-chromosphere boundary where the cut-off frequency takes effect. The presentation of quiescent wave power consistent with previous works (Jess et al., 2023b, see) reassures that the data products and analysis techniques are valid, and the magnetic wave configurations observed are reliable.

4 Discussions and conclusion

Many authors have studied the propagation of waves in the solar atmosphere, observing either propagating or standing waves, usually probing only a few spectral lines to provide a multi-height analysis. Here, utilising the FRANCIS instrument, we studied, for the first time, the vertical modulation of oscillations throughout the lower solar atmosphere using 21 different spectral lines. The high spatial and spectral resolution achieved by FRANCIS allowed us to study the behaviour of distinct magnetised regions within an active region at heights ranging from ~10 to ~400 km above the photosphere, uncovering various wave populations.

Figures 2, 4 show the spectral power observed in both the plage and sunspot fibres as a function of height. Focussing first on the plage region, we do not observe the increase of power dominance from 3 mHz towards 5 mHz (Jess et al., 2023b) in the quiet Sun acoustic oscillations expected of large height

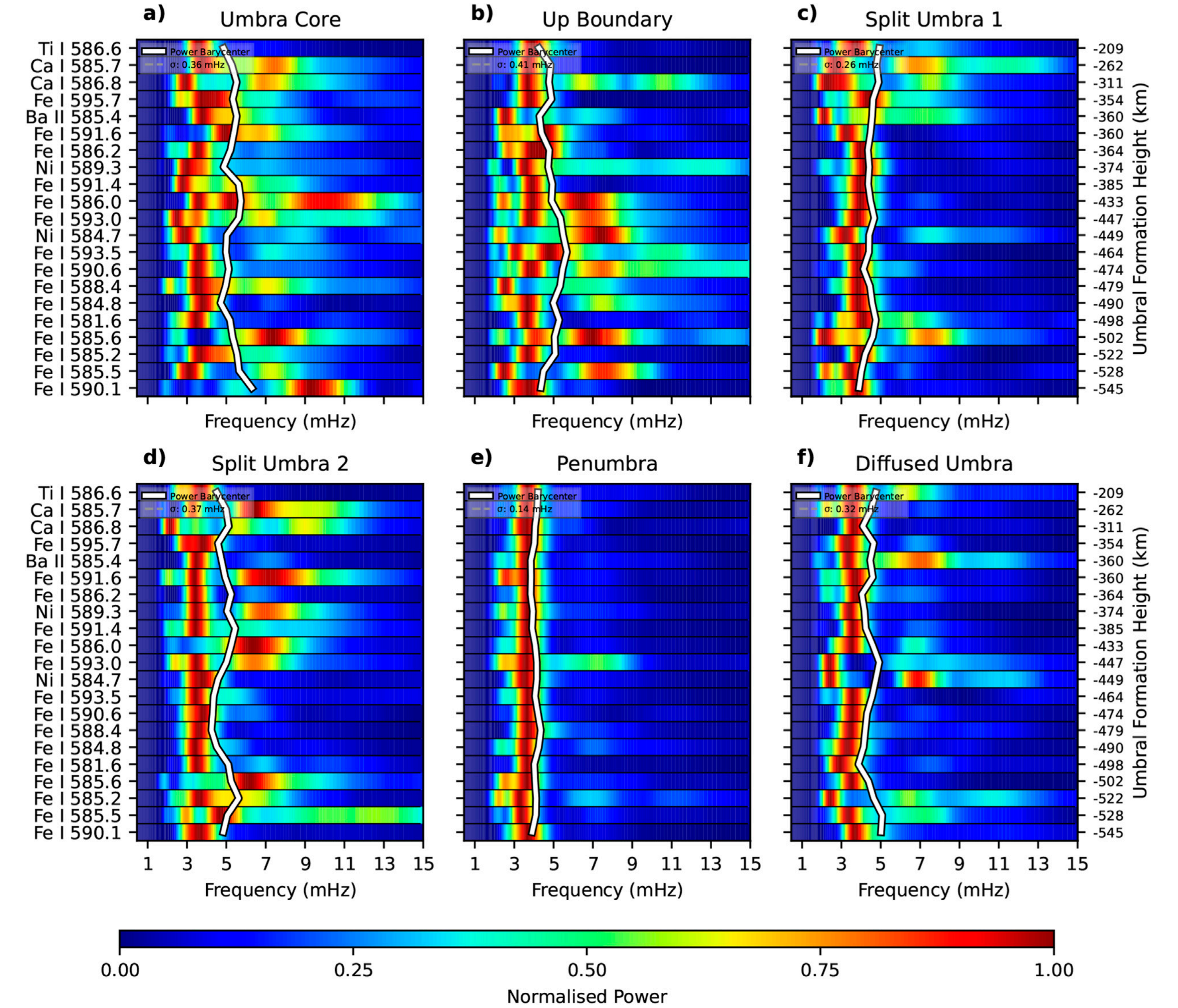

FIGURE 2
RGWSs as a function of frequency and height for the six differently magnetised regions of the AR considered in this work. The left vertical axis lists the specific spectral lines analysed, while the right vertical axis displays the approximate formation heights in km. Note the different spectral features characterising wave populations at different heights. The white line in each panel traces the frequency-weighted mean power, and its amplitude is reported in the legend. **(a)** Umbra Core. **(b)** Up Boundary. **(c)** Split Umbra 1. **(d)** Split Umbra 2. **(e)** Penumbra. **(f)** Diffused Umbra.

differentials. It is worth emphasising that our diagnostics sample a comparatively narrow height range confined to the upper photosphere (~10–400 km), whereas many multi-line studies extend much higher into the chromosphere (e.g., quiet-Sun IRIS analyses such as Kayshap et al. 2025), where the 3–5 mHz filtering is more readily observed; differences in magnetic environment (quiet Sun versus plage) may further modify the effective cut-off and its observational signature. Indeed, depending on magnetic field strength and inclination, as well as radiative losses, the effective cut-off frequency can be modified. Furthermore, given the short duration of our observations, evanescent waves below the cut-off could still leave a trace in the RGWS. It is also worth noting that other diagnostic-related effects, such as the velocity response of the lines, could alter the estimated vertical ordering, complicating any further interpretation related to the propagation of waves.

Apart from instrumental and diagnostic-related biases, other physical mechanisms could also influence the behaviour and oscillations observed in the plage regions. First, the proximity of the sunspot, which oscillates at the same frequency but is less susceptible to the acoustic cut-off due to the magnetic nature of converted modes, could cause deviations from the expected behaviour. Additionally, as seen in Figure 3 of Jess et al. (2013), more inclined magnetic field lines facilitate the propagation of different frequencies, contributing to the behaviour observed in the regions analysed here. Finally, the atmospheric heights explored in this work remain largely photospheric, with the highest level just reaching the boundary layer with the chromosphere.

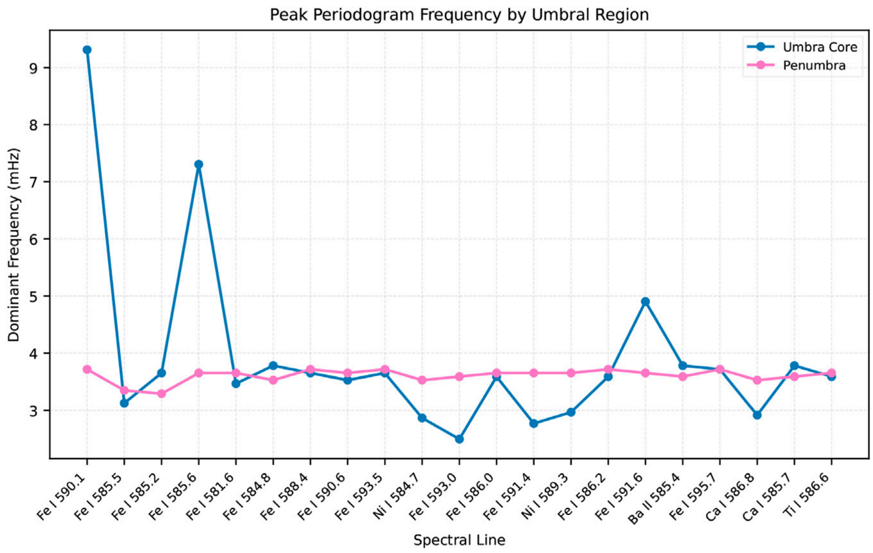

FIGURE 3
The dominant frequency within the umbral core and penumbral fibre for each spectral line, arranged in height-ascending order for a magnetic region.

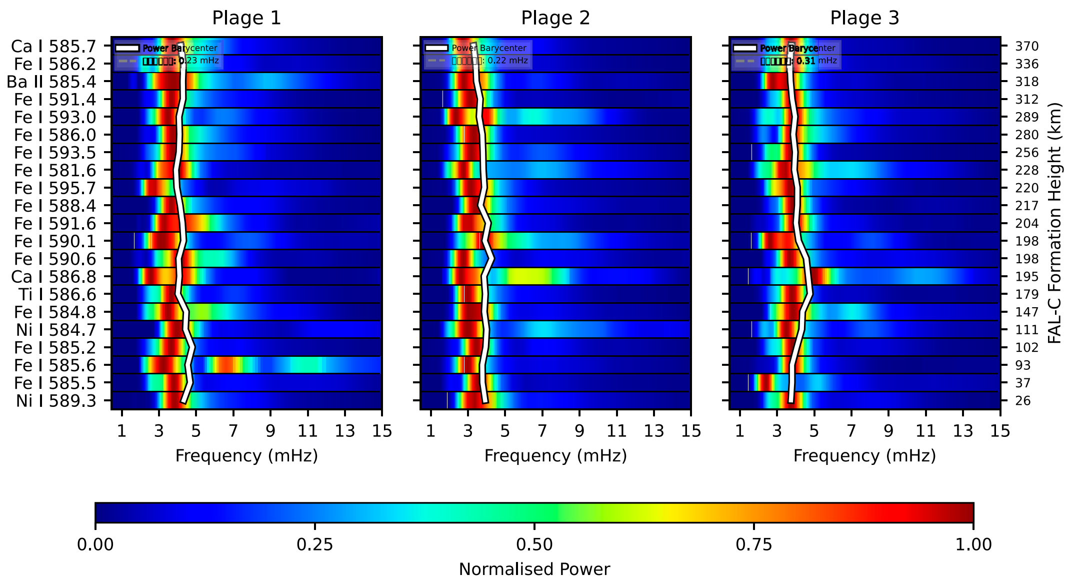

FIGURE 4
RGWSs as a function of frequency and height for the three plage region fibres of the AR considered in this work. The left side of the vertical axis lists the specific spectral lines analysed, while the right side displays the approximate formation heights in km. The white line in each panel traces the frequency-weighted mean power, and its amplitude is reported in the legend.

Conversely, Figure 2 shows a strikingly different scenario for the sunspot fibres. Spectral features at higher frequencies are more common at all heights, further highlighting how the magnetic field topology, inclination, and other plasma parameters drive the dynamics of the solar atmosphere. Distinct neighbouring regions within the same active region contain different wave populations, an effect that becomes even more apparent at greater heights where inclined fields can cross the line of sight and alter the observed wave signature. Beyond the high-frequency range, the 3 – 4 mHz band remains the most prominent spectral feature across all fibres, despite presenting a more dynamic behaviour. The 3 – 4 mHz peaks are narrower and slightly shifted towards higher frequencies, which consistent with magneto-acoustic mode conversion in structured magnetic atmospheres (e.g., Spruit and Bogdan, 1992; Cally et al., 1994). In an analogy with a string instrument, here the magnetic field contributes to the restoring forces, causing a shift towards higher frequencies as the tension increases. However, quantitative analysis of this effect is currently constrained by our frequency resolution, so whilst large frequency shifts in power between 3 and 5 mHz are detectable, fine-scale transitions may remain beyond our observations. Future observing campaigns of longer durations will allow for small shifts in wave power across frequencies to be positively identified. It is also clear that within the height range sampled by these lines, the dominant frequency shift from 3 to 5 mHz (as a function of height) is not clearly seen. Previous studies were able to resolve a clear shift to higher frequencies with height, however, they often sampled far larger height ranges and given that our derived heights are first-order approximations, more intensive height synthesis would be required to fully resolve the height-dependent wave power structuring.

The initial results obtained with FRANCIS demonstrate the capability of simultaneous multi-line IFU spectroscopy to (i) capture a largely persistent 3–4 mHz power concentration across the sampled upper-photospheric heights, (ii) reveal pronounced region-to-region variability within the same active region–including enhanced high-frequency power in selected umbral components–and (iii) show that, within the comparatively narrow height range sampled here (~10–400 km), the canonical height-dependent shift of dominance from ~3 mHz toward ~5 mHz is not clearly expressed in the penumbral and plage fibres, while some of the spectral lines in the umbral components exhibit substantial power at higher frequencies already within the sampled photospheric layers. By selecting individual sample fibres, we were able to showcase the distinct behaviours of the umbra, umbra-penumbra boundary, penumbra, and plage. The line-dependent appearance of higher frequency wave power within the umbra is in qualitative agreement with recent sunrise III/SUSI studies(Korpi-Lagg et al., 2025; Feller et al., 2025; Solanki et al., 2026), which found both strong line-to-line differences in the umbral frequency spectra and a clear environment-dependent redistribution of oscillatory power across active-region structures in seeing-free, near-UV observations (Jafarzadeh et al., 2026b; Jafarzadeh et al., 2026c). These results highlight the significant spatial variability of wave modes and highlight the importance of future studies linking this variability to other plasma parameters, such as magnetic field inclination angles derived from extrapolations. Upcoming upgrades to the instrument will enable full polarimetric observations, aiding in determining the nature of the observed waves and offering new insights into mode conversion across different heights. FRANCIS, and IFUs more broadly, are set to become valuable tools for a better understanding of wave dynamics in the solar atmosphere.

Data availability statement

The raw data supporting the conclusions of this article will be made available by the authors, without undue reservation.

Author contributions

SG: Data curation, Methodology, Investigation, Formal Analysis, Validation, Visualization, Writing – original draft, Project administration. MB: Formal Analysis, Software, Writing – original draft, Visualization, Investigation, Data curation, Methodology. GC: Data curation, Investigation, Software, Validation, Writing – original draft. DBJ: Data Curation, Conceptualization, Supervision, Writing – original draft. MS: Conceptualization, Investigation, Validation, Supervision, Writing – original draft. SJ: Visualization, Validation, Software, Methodology, Writing – original draft, Investigation. HS: Software, Formal Analysis, Methodology, Writing – original draft. FB: Validation, Resources, Supervision, Writing – original draft.

Funding

The author(s) declared that financial support was received for this work and/or its publication. SG, GC, DJ, and SJ wish to thank the United Kingdom Science and Technology Facilities Council (STFC) for the consolidated grants ST/T00021X/1 and ST/X000923/1, alongside the PATT Travel Grant UKRI372. SG and DJ also acknowledge funding from the United Kingdom Space Agency via the National Space Technology Programme (grant SSc-009). MB acknowledges that this publication (communication/thesis/article, etc.) was produced while attending the PhD programme in PhD in Space Science and Technology at the University of Trento, Cycle XXXIX, with the support of a scholarship financed by the Ministerial Decree no. 118 of 2 March 2023, based on the NRRP - funded by the European Union - NextGenerationEU - Mission 4 “Education and Research,” Component 1 “Enhancement of the offer of educational services: from nurseries to universities” - Investment 4.1 “Extension of the number of research doctorates and innovative doctorates for public administration and cultural heritage” - CUP E66E23000110001. DJ acknowledges support from the Leverhulme Trust via the Research Project Grant RPG-2019-371. SJ acknowledges support from the Rosseland Centre for Solar Physics, University of Oslo, Norway. We wish to acknowledge scientific discussions with the Waves in the Lower Solar Atmosphere (WaLSA; www.WaLSA.team) team, which has been supported by the Research Council of Norway (project no. 262622), The Royal Society (award no. Hooke18b/SCTM; Jess et al., 2021b), and the International Space Science Institute (ISSI) in Bern through ISSI International Team project 502 “WaLSA: Waves in the Lower Solar Atmosphere at High Resolution”.

Conflict of interest

The author(s) declared that this work was conducted in the absence of any commercial or financial relationships that could be construed as a potential conflict of interest.

The Reviewer JS declared a past collaboration with the author(s) DJ to the Handling Editor at the time of review.

Generative AI statement

The author(s) declared that generative AI was not used in the creation of this manuscript.

Any alternative text (alt text) provided alongside figures in this article has been generated by Frontiers with the support of artificial intelligence and reasonable efforts have been made to ensure accuracy, including review by the authors wherever possible. If you identify any issues, please contact us.

Publisher's note

All claims expressed in this article are solely those of the authors and do not necessarily represent those of their affiliated organizations, or those of the publisher, the editors and the reviewers. Any product that may be evaluated in this article, or claim that may be made by its manufacturer, is not guaranteed or endorsed by the publisher.

References

Bahauddin, S. M., Fischer, C. E., Rast, M. P., Milic, I., Woeger, F., Rempel, M., et al. (2024). Observations of locally excited waves in the low solar atmosphere using the daniel K. Inouye solar telescope. *Astrophysical J.* 971, L1. doi:10.3847/2041-8213/ad62f8

BASS2000 (2001). Solar spectrum. Available online at: https://bass2000.obspm.fr/solar_spect.php.ObservatoiredeParis/BASS2000 (Accessed October 2, 2025).

Bogdan, T. J. (2000). Sunspot oscillations: a review - (invited review). *Sol. Phys.* 192, 373–394. doi:10.1023/A:1005225214520

Bogdan, T., and Judge, P. (2006). Observational aspects of sunspot oscillations. *Philosophical Trans. R. Soc. A Math. Phys. Eng. Sci.* 364, 313–331. doi:10.1098/rsta.2005.1701

Bogdan, T. J., Hansteen, M. C. V., McMurry, A., Rosenthal, C. S., Johnson, M., Petty-Powell, S., et al. (2003). Waves in the magnetized solar atmosphere. II. Waves from localized sources in magnetic flux concentrations. *Astrophysical J.* 599, 626–660. doi:10.1086/378512

Brown, T. M. (1986). "Measuring the Sun's internal rotation using solar p-mode oscillations," in *Seismology of the Sun and the Distant Stars*. Editor D. O. Gough (NATO Advanced Study Institute (ASI) Series C) 169, 199–214.

Cally, P. S., Bogdan, T. J., and Zweibel, E. G. (1994). Umbral oscillations in sunspots: absorption of p-modes and active region heating by mode conversion. *Astrophysical J.* 437, 505. doi:10.1086/175014

Cavallini, F. (2006). IBIS: a new post-focus instrument for solar imaging spectroscopy. *Sol. Phys.* 236, 415–439. doi:10.1007/s11207-006-0103-8

Centeno, R., Collados, M., and Bueno, J. T. (2006). Oscillations and wave propagation in different solar magnetic features, 465.

Centeno, R., Collados, M., and Trujillo Bueno, J. (2009). Wave propagation and shock formation in different magnetic structures. 692, 1211–1220. doi:10.1088/0004-637X/692/2/1211692.1211C

Chambers, G., Jess, D. B., Jafarzadeh, S., Berretti, M., Grant, S. D. T., Stangalini, M., et al. (2026). Standing oscillations in a resonant sunspot atmosphere captured by integral field spectroscopy. *Front. in Astronomy and Space Sci. Under Review*. doi:10.48550/arXiv.2606.25217

Chaturmutha, V., Fleck, B., and Jefferies, S. M. (2024). Wave reflection in the solar atmosphere. *Astrophysical J.* 966, 200. doi:10.3847/1538-4357/ad36c5

Doorsselaere, T. V., Srivastava, A. K., Antolin, P., Magyar, N., Farahani, S. V., Tian, H., et al. (2020). Coronal heating by MHD waves. *Space Sci. Rev.* 216, 140. doi:10.1007/s11214-020-00770-y

Dorotovič, I., Erdélyi, R., Freij, N., Karlovský, V., and Márquez, I. (2014). Standing sausage waves in photospheric magnetic waveguides. *Astronomy and Astrophysics* 563, A12. doi:10.1051/0004-6361/201220542

D'Silva, S. (1994). Acoustic mode mixing in sunspots. *Astrophysical J.* 435, 881. doi:10.1086/174869

Edwin, P. M., and Roberts, B. (1982). Wave propagation in a magnetically structured atmosphere. *Sol. Phys.* 76, 239–259. doi:10.1007/bf00170986

Edwin, P. M., and Roberts, B. (1983). Wave propagation in a magnetic cylinder. *Sol. Phys.* 88, 179–191. doi:10.1007/bf00196186

Evans, J. (1981). Solar instrumentation: what's next?

Fedun, V., Shelyag, S., Verth, G., Mathioudakis, M., and Erdélyi, R. (2011). MHD waves generated by high-frequency photospheric vortex motions. *Ann. Geophys.* 29, 1029–1035. doi:10.5194/angeo-29-1029-2011

Feller, A., Gandorfer, A., Grauf, B., Hölken, J., Iglesias, F. A., Korpi-Lagg, A., et al. (2025). The sunrise ultraviolet spectropolarimeter and imager: instrument description. 300, 65. doi:10.1007/s11207-025-02471-765F

Fleck, B., and Deubner, F. L. (1989). Dynamics of the solar atmosphere. II - standing waves in the solar chromosphere. *Astronomy Astrophysics* 224, 245–252.

Fontenla, J. M., Avrett, E. H., and Loeser, R. (1993). Energy balance in the solar transition region. III. Helium emission in hydrostatic. *Constant-Abundance Models Diffusion* 406, 319. doi:10.1086/172443

Forte, R., Jefferies, S. M., Berrilli, F., Del Moro, D., Fleck, B., Giovannelli, L., et al. (2018). "The MOTH II doppler-magnetographs and data calibration pipeline," in *Space Weather of the Heliosphere: Processes and Forecasts*. Editors C. Foullon, and O. E. Malandraki, 335–339. doi:10.1017/S1743921318000029

Gilchrist-Millar, C. A., Jess, D. B., Grant, S. D. T., Keys, P. H., Beck, C., Jafarzadeh, S., et al. (2021). Magnetoacoustic wave energy dissipation in the atmosphere of solar pores. *Philosophical Trans. R. Soc. A* 379, 20200172. doi:10.1098/rsta.2020.0172

Giovanelli, R. G., Harvey, J. W., and Livingston, W. C. (1978). Motions in solar magnetic tubes. *Sol. Phys.* 58, 347–361. doi:10.1007/bf00157281

Goossens, M., Doorsselaere, T. V., Soler, R., and Verth, G. (2013). Energy content and propagation in transverse solar atmospheric waves. *Astrophysical J.* 768, 191. doi:10.1088/0004-637x/768/2/191

Grant, S. D. T., Jess, D. B., Moreels, M. G., Morton, R. J., Christian, D. J., Giagkiozis, I., et al. (2015). Wave damping observed in upwardly propagating sausage-mode oscillations contained within a magnetic pore. *Astrophysical J.* 806, 132. doi:10.1088/0004-637x/806/1/132

Grant, S. D. T., Jess, D. B., Stangalini, M., Jafarzadeh, S., Fedun, V., Verth, G., et al. (2022). The propagation of coherent waves across multiple solar magnetic pores. *Astrophysical J.* 938, 143. doi:10.3847/1538-4357/ac91ca

Iglesias, F. A., and Feller, A. (2019). Instrumentation for solar spectropolarimetry: state of the art and prospects. *Opt. Eng.* 58, 082417. doi:10.1117/1.OE.58.8.082417

Jaeggli, S. A., Lin, H., Mickey, D. L., Kuhn, J. R., Hegwer, S. L., Rimmele, T. R., et al. (2010). FIRS: a new instrument for photospheric and chromospheric studies at the DST. *Mem. Soc. Astron. Ital.* 81, 763.

Jafarzadeh, S., Solanki, S. K., Gafeira, R., Noort, M. v., Barthol, P., Rodríguez, J. B., et al. (2017). Transverse oscillations in slender Ca ii H fibrils observed with Sunrise/SuFI. *Astrophysical J. Suppl. Ser.* 229, 9. doi:10.3847/1538-4365/229/1/9

Jafarzadeh, S., Wedemeyer, S., Fleck, B., Stangalini, M., Jess, D. B., Morton, R. J., et al. (2021). An overall view of temperature oscillations in the solar chromosphere with ALMA. *Philosophical Trans. R. Soc. A* 379, 20200174. doi:10.1098/rsta.2020.0174

Jafarzadeh, S., Jess, D. B., Stangalini, M., Grant, S. D. T., Higham, J. E., Pessah, M. E., et al. (2025). enWave analysis tools. *Nat. Rev. Methods Prim.* 5, 21. doi:10.1038/s43586-025-00392-0

Jafarzadeh, S., Jess, D. B., Stangalini, M., Keys, P. H., Chambers, G., Grant, S. D. T., et al. (2026a). Adaptive multi-line fitting for stable line-core intensity and doppler velocity. *Front. in Astronomy and Space Sci.* 13. doi:10.3389/fspas.2026.1843842

Jafarzadeh, S., Jess, D. B., Stangalini, M., Keys, P. H., Grant, S. D. T., Duckenfield, T. J., et al. (2026b). Magnetically structured oscillatory power along an active-region transect in Near-UV sunrise iii/SUSI spectroscopy.

Jafarzadeh, S., Jess, D. B., Stangalini, M., Morton, R. J., Felipe, T., Berretti, M., et al. (2026c). "Multi-line wave signatures in a sunspot from Near-UV sunrise iii/SUSI observations," in *Prep. (Focus Issue on Early Science Results from Sunrise Iii)*.

Jefferies, S. M., Osaki, Y., Shibahashi, H., Harvey, J. W., D'Silva, S., and Duvall, T. L., Jr. (1997). Sounding the sun's chromosphere. *Astrophysical J.* 485, L49–L52. doi:10.1086/310805

Jefferies, S. M., Fleck, B., Murphy, N., and Berrilli, F. (2019). Observed local dispersion relations for magnetoacoustic-gravity waves in the sun's atmosphere: mapping the Acoustic cutoff frequency. *Astrophysical J. Lett.* 884, L8. doi:10.3847/2041-8213/ab4719

Jess, D. B., Mathioudakis, M., Christian, D. J., Keenan, F. P., Ryans, R. S. I., and Crockett, P. J. (2010). ROSA: a high-cadence, synchronized multi-camera solar imaging system. *Sol. Phys.* 261, 363–373. doi:10.1007/s11207-009-9500-0

Jess, D. B., Moortel, I. D., Mathioudakis, M., Christian, D. J., Reardon, K. P., Keys, P. H., et al. (2012). The source of 3 minute magnetoacoustic oscillations in coronal fans. *Astrophysical J.* 757, 160. doi:10.1088/0004-637x/757/2/160

Jess, D. B., Reznikova, V. E., Doorsselaere, T. V., Keys, P. H., and Mackay, D. H. (2013). The influence of the magnetic field on running penumbral waves in the solar chromosphere. *Astrophysical J.* 779, 168. doi:10.1088/0004-637x/779/2/168

Jess, D. B., Keys, P. H., Stangalini, M., and Jafarzadeh, S. (2021a). High-resolution wave dynamics in the lower solar atmosphere. *Philosophical Trans. R. Soc. Lond. Ser. A* 379, 20200169. doi:10.1098/rsta.2020.0169

Jess, D. B., Snow, B., Fleck, B., Stangalini, M., and Jafarzadeh, S. (2021b). Reply to: signatures of sunspot oscillations and the case for chromospheric resonances. *Nat. Astron.* 5, 5–8. doi:10.1038/s41550-020-1158-4

Jess, D. B., Grant, S. D. T., Bate, W., Liu, J., Jafarzadeh, S., Keys, P. H., et al. (2023a). The fibre resolved OpticAl and near-ultraviolet czerny-turner imaging spectropolarimeter (FRANCIS). *Sol. Phys.* 298, 146. doi:10.1007/s11207-023-02237-z

Jess, D. B., Jafarzadeh, S., Keys, P. H., Stangalini, M., Verth, G., and Grant, S. D. T. (2023b). Waves in the lower solar atmosphere: the dawn of next-generation solar telescopes. *Living Rev. Sol. Phys.* 20, 1. doi:10.1007/s41116-022-00035-6

Jones, H. P. (1989). Formation of fourier phase shifts in the solar Ni i 6768 Å line. *Sol. Phys.* 120, 211–234. doi:10.1007/BF00159876

Kayshap, P., Murawski, K., Srivastava, A. K., Musielak, Z. E., and Dwivedi, B. N. (2018). Vertical propagation of Acoustic waves in the solar internetworkas observed by IRIS. *Mon. Notices R. Astronomical Soc.* 479, 5512–5521. doi:10.1093/mnras/sty1861

Kayshap, P., Srivastava, A. K., Tiwari, S. K., Jelínek, P., and Mathioudakis, M. (2020). Propagation of waves above a plage as observed by IRIS and SDO. 634, A63. doi:10.1051/0004-6361/201936070634A63K

Kayshap, P., Murawski, K., Musielak, Z. E., and Babu, B. S. (2025). Variations in dominant wave period in the solar atmosphere. *Astrophys. J.* 987, 161. doi:10.3847/1538-4357/ade14e

Khomenko, E., and Collados, M. (2009). Sunspot seismic halos generated by fast MHD wave refraction. *Astronomy Astrophysics* 506, L5–L8. doi:10.1051/0004-6361/200913030

Khomenko, E., Centeno, R., Collados, M., and Bueno, J. T. (2008). Channeling 5 minute photospheric oscillations into the solar outer atmosphere through small-scale vertical magnetic flux tubes. *Astrophysical J. Lett.* 676, L85–L88. doi:10.1086/587057

Kneer, F., Mattig, W., and v. Uexkuell, M. (1981). The chromosphere above sunspot umbrae. III - spatial and temporal variations of chromospheric lines. *Astronomy Astrophysics* 102, 147–155.

Korpi-Lagg, A., Gandorfer, A., Solanki, S. K., del Toro Iniesta, J. C., Katsukawa, Y., Bernasconi, P., et al. (2025). SUNRISE III: overview of observatory and instruments. 300, 75. doi:10.1007/s11207-025-02485-175K

Krishna Prasad, S., Jess, D. B., and Khomenko, E. (2015). On the source of propagating slow magnetoacoustic waves in sunspots. 812, L15. doi:10.1088/2041-8205/812/1/L15812L15K

Krishna Prasad, S., Jess, D. B., Van Doorsselaere, T., Verth, G., Morton, R. J., Fedun, V., et al. (2017). The frequency-dependent damping of slow magnetoacoustic waves in a sunspot umbral atmosphere. 847, 5. doi:10.3847/1538-4357/aa86b5847

Lites, B. W. (1984). Photoelectric observations of chromospheric sunspot oscillations. II - Propagation characteristics. *Astrophysical J.* 277, 874. doi:10.1086/161758

Lites, B. W. (1986). Photoelectric observations of chromospheric sunspot oscillations. IV. The CA II H lines and he i lambda 10830. *Astrophysical J.* 301, 1005. doi:10.1086/163964

Lites, B. W. (1992). Sunspot oscillations - observations and implications. 375, 261. 302. doi:10.1007/978-94-011-2769-1_12

Lites, B. W., and Thomas, J. H. (1985). Sunspot umbral oscillations in the photosphere and low chromosphere. *Astrophysical J.* 294, 682. doi:10.1086/163338

Löhner-Böttcher, J., and Bello González, N. (2015). Signatures of running penumbral waves in sunspot photospheres. 580. doi:10.1051/0004-6361/201526230 580A53L

Löhner-Böttcher, J., Bello González, N., and Schmidt, W. (2016). Magnetic field reconstruction based on sunspot oscillations. *Astron. Nachrichten* 337, 1040. doi:10.1002/asna.2016124303371040L

Mein, N., and Mein, P. (1976). Velocity waves in the quiet solar chromosphere. *Sol. Phys.* 49, 231–248. doi:10.1007/bf00162447

Moretti, P. F., Jefferies, S. M., Armstrong, J. D., and Intosh, S. W. M. (2007). Observational signatures of the interaction between Acoustic waves and the solar magnetic canopy. *Astronomy and Astrophysics* 471, 961–965. doi:10.1051/0004-6361:20077247

Pesnell, W. D., Thompson, B. J., and Chamberlin, P. C. (2012). The solar dynamics observatory (SDO). *Sol. Phys.* 275, 3–15. doi:10.1007/s11207-011-9841-3

Pontieu, B. D., McIntosh, S. W., Carlsson, M., Hansteen, V. H., Tarbell, T. D., Schrijver, C. J., et al. (2007). Chromospheric alfvénic waves strong enough to power the solar wind. *Science* 318, 1574–1577. doi:10.1126/science.1151747

Provost, J., and Mein, N. (1979). enWave reflections in the solar atmosphere. *Sol. Phys.* 64, 43–56. doi:10.1007/BF00151114

Rempel, M. (2012). Numerical sunspot models: robustness of photospheric velocity and magnetic field structure. *Astrophys. J.* 750, 62. doi:10.1088/0004-637X/750/1/62

Rijs, C., Moradi, H., Przybylski, D., and Cally, P. S. (2015). MHD wave refraction and the Acoustic halo effect around solar active regions: a 3D study. *Astrophysical J.* 801, 27. doi:10.1088/0004-637X/801/1/27

Roberts, B. (2019). *Enmhd Waves in the Solar Atmosphere*.

Rosenthal, C. S., Bogdan, T. J., Carlsson, M., Dorch, S. B. F., Hansteen, V., McIntosh, S. W., et al. (2002). Waves in the magnetized solar atmosphere. I. Basic processes and internetwork oscillations. *Astrophysical J.* 564, 508–524. doi:10.1086/324214

Rutten, R. J. (2021). Compendium solar spectrum formation. *arXiv e-prints, arXiv:2103.02369*. doi:10.48550/arXiv.2103.02369

Schlichenmaier, R., and Schmidt, W. (2000). Flow geometry in a sunspot penumbra. *Astronomy Astrophysics* 358, 1122–1132.

Schou, J., Scherrer, P. H., Bush, R. I., Wachter, R., Couvidat, S., Rabello-Soares, M. C., et al. (2012). Design and ground calibration of the helioseismic and magnetic imager (HMI) instrument on the solar dynamics observatory (SDO). *Sol. Phys.* 275, 229–259. doi:10.1007/s11207-011-9842-2

Smitha, H. N., van Noort, M., Solanki, S. K., and Castellanos Durán, J. S. (2023). Non-LTE formation of the Fe I 6173 Å line in the solar atmosphere. *Astron. Astrophys.* 669, A144. doi:10.1051/0004-6361/202245130

Socas-Navarro, H., Bueno, J. T., and Cobo, B. R. (2000). Anomalous polarization profiles in sunspots: possible origin of umbral flashes. *Science* 288, 1396–1398. doi:10.1126/science.288.5470.1396

Solanki, S. K. (2003). Sunspots: an overview. *Astron. Astrophys. Rev.* 11, 153–286. doi:10.1007/s00159-003-0018-4

Solanki, S. K., Smitha, H. N., Lagg, A., Gandorfer, A., del Toro Iniesta, J. C., Katsukawa, Y., et al. (2026). “Sunrise iii: instrument, mission, data, and first results,” in *Prep. (Focus Issue on Early Science Results from Sunrise Iii)*.

Spruit, H. C. (1981). Motion of magnetic flux tubes in the solar convection zone and chromosphere. *Astronomy and Astrophysics* 98, 155–160.

Spruit, H. C., and Bogdan, T. J. (1992). The conversion of p-modes to slow modes and the absorption of Acoustic waves by sunspots. *Astrophysical J.* 391, L109. doi:10.1086/186409

Stangalini, M., Jess, D. B., Verth, G., Fedun, V., Fleck, B., Jafarzadeh, S., et al. (2021). enA novel approach to identify resonant MHD wave modes in solar pores and sunspot umbrae: b analysis. *Astronomy and Astrophysics* 649, A169. doi:10.1051/0004-6361/202140429

Vigeesh, G., Steiner, O., and Hasan, S. S. (2011). Stokes diagnostics of magneto-acoustic wave propagation in the magnetic network on the sun. *Sol. Phys.* 273, 15–38. doi:10.1007/s11207-011-9851-1

Zhugzhda, Y. D. (1984). Resonance oscillations in sunspots and transformation of magneto-acoustic-gravity waves. *Mon. Notices R. Astronomical Soc.* 207, 731–744. doi:10.1093/mnras/207.4.731